Continuous symmetry maps and shape classification. The case of six-coordinated metal compounds†

Santiago Alvarez,[ab] David Avnir,[c] Miquel Llunell[bd] and Mark Pinsky[ce]

[a] *Departament de Química Inorgànica, Universitat de Barcelona Diagonal 647, 08028, Barcelona, Spain. E-mail: santiago@qi.ub.es*
[b] *Centre de Recerca en Química Teòrica, Parc Científic de Barcelona Baldiri i Reixach 11, 08028, Barcelona, Spain*
[c] *Institute of Chemistry and The Lise Meitner Minerva Center for Computational Quantum Chemistry, The Hebrew University of Jerusalem, Jerusalem 91904, Israel*
[d] *Departament de Química Física, Universitat de Barcelona, Diagonal 647, 08028 Barcelona, Spain*
[e] *Institute of Earth Sciences, The Hebrew University of Jerusalem, Jerusalem 91904, Israel*

Received (in Montpellier, France) 7th January 2002, Accepted 12th March 2002
First published as an Advance Article on the web

A continuous symmetry study of the structures of transition metal six-vertex polyhedra is presented, considering both molecular models and experimental structural data. The concept of symmetry map is introduced, consisting of a scatterplot of the symmetry measures relative to two alternative ideal polyhedra. In the case of hexacoordinated complexes, we take as reference shapes the octahedron and the equilateral trigonal prism and study different distortions from these two extremes, including the Bailar twist that interconverts one into another. Such a symmetry map allows us to establish trends in the structural chemistry of the coordination sphere of hexacoordinated transition metal atoms, including the effects of several factors, such as the electron configuration or the presence of bidentate, terdentate or encapsulating ligands. Also introduced is the concept of a *symmetry constant*, which identifies a distortive route that preserves the minimum distance to two reference symmetries. A wide variety of model distortions are analyzed, and the models are tested against experimental structural data of a wide variety of six-coordinated complexes.

One of the most useful and widespread idealizations of molecular structures consists in associating the position of a set of atoms with the vertices of a reference polyhedron. An accurate description of the structure of a molecule, though, often requires the use of qualifiers such as *slightly distorted* or *severely distorted* relative to the reference polyhedron. We also often describe a structure as *intermediate* between two alternative polyhedra. To quantify the degree of distortion of a particular molecular structure from an ideal polyhedron one can use *symmetry measures* as defined, for instance, by Avnir and coworkers.[1] This symmetry measure determines the *distance* of a structure from the perfect symmetry of a given point group or from a reference shape. In the chemistry of transition metal compounds, the most ubiquitous polyhedron is probably the octahedron, whose vertices describe the positions of the donor atoms in a hexacoordinated complex ML_6, as well as the environment of transition metal atoms in a wide variety of extended solids. The same polyhedron can be used to define the position of six metal atoms in M_6L_n clusters with metal-metal bonds, or in hexanuclear supramolecular assemblies in which the metal atoms are farther apart and held together by bridging ligands. We restrict the present study to molecular ML_6 groups but the general approach described below is applicable to other specific families of six-vertex polyhedral structures.

An alternative coordination polyhedron, the trigonal prism, is not unusual and can be found in solids with the MoS_2- or WC-type structures, in several tris(dithiolene) complexes, hexamethyl compounds, some complexes with encapsulating ligands or in porphyrin and phthalocyanine complexes of early transition metals. According to theoretical studies carried out by several authors on methyl[2–4] and hydrido[5] homoleptic complexes, hexacoordinated d^0 and d^1 complexes should be trigonal prismatic rather than octahedral, with an additional distortion to C_{3v} due to a second order Jahn–Teller effect. Besides the fundamental interest in the structural choice between octahedron and trigonal prism, boosted in recent years by the theoretical prediction and experimental report of trigonal prismatic hexa(methyl) complexes,[2–4,6–10] the interconversion of the two polyhedra has been proposed to be operative in the trigonal twist described early on by Bailar[11] as a pathway for the racemization reaction of tris(chelate) complexes.

The general problem we face is to decide (*a*) which is the polyhedron or polygon that best describes the geometry of the set of atoms under consideration, (*b*) how far is the real structure from such an ideal geometry and (*c*) how to recognize automatically if the six-coordinated compound under investigation is best represented by other less common polyhedra, such as the pentagonal pyramid or the hexagon. The continuous symmetry measures approach allows one to answer the second question once a reference geometry has been selected. But so far the selection of a reference shape is made based mostly on visual inspection of a structure, on the knowledge of structures of related compounds, or on the comparison of the bonding parameters (bond distances, bond angles and torsion angles) with those of the reference shape. The number and nature of parameters that must be analyzed to discriminate

† Electronic supplementary information (ESI) available: tables of CSD refcodes, structural parameters and symmetry measures for the studied compounds. See http://www.rsc.org/suppdata/nj/b2/b202096n/

 DOI: 10.1039/b200641n

between two alternative structures depends on the specific shapes considered and increases with the number of vertices.[12] Therefore, it is not easy to establish an algorithm that allows one to decide, based on a small number of bonding parameters that are common to all of the polyhedra considered, whether a set of, say, six ligands is best described as an octahedron, a trigonal prism, a hexagon, a pentagonal pyramid or some other shape. In this paper we will show how the analysis of just two symmetry measures for six-vertex polyhedra provides indications of the most likely shapes and how in some instances it provides a unique identification of the closest polyhedron.

The polyhedral-symmetry measurement methodology

In the past several years we have developed a general methodology for measuring, on a quantitative scale, the degree of symmetry (and chirality) content in a given (distorted) structure.[1,13] Many novel correlations between symmetry or chirality and molecular properties have been consequently revealed.[14–20] The measure, which seeks the minimal distance to the desired perfect symmetry, has been backed both by a general algorithm and by several specific algorithms and computational tools tailored for specific needs, including a computer code suitable for the family of the regular and semiregular polyhedra. Such a tool allows not only the determination of the *distance* of a molecular structure to a given ideal polyhedron—the original task for which it was developed—but it also allows the quantitative evaluation of the contents of any given shape, symmetric or not, in any structure.

According to the continuous symmetry measures (CSM) methodology, given a structure composed of N vertices whose coordinates are given by the vectors Q_k ($k = 1, 2 \ldots N$), one searches for a perfectly G-symmetric object (G being a specific symmetry group) with coordinates P_k ($k = 1, 2 \ldots N$). One then calculates the distances between the vertices of the two objects and repeats the search until a set of P_k coordinates is found that minimizes the distances, according to eqn. (1) (where Q_0 is the coordinate vector of the center of mass of the investigated structure and the denominator is a size normalization factor):

$$S(\mathrm{G}) = \min \frac{\sum_{k=1}^{N} |Q_k - P_k|^2}{\sum_{k=1}^{N} |Q_k - Q_0|^2} \cdot 100 \qquad (1)$$

The resulting value of S(G) is the G symmetry measure of the investigated structure (Q_k) and in the process one obtains also the closest structure with perfect G symmetry (P_k).

The symmetry measures defined in eqn. (1) must lie within the range $100 \geqslant S \geqslant 0$. If a structure has the desired G-symmetry, $S(\mathrm{G}) = 0$ and the symmetry measure increases as it departs from G-symmetry, reaching a maximum value (not necessarily 100).[20] All S(G) values, regardless of G, are on the same scale, a property that allows one to compare, for example, the degree of octahedricity and D_{3h}-ness of various distorted octahedral complexes. A set of programs has been developed in recent years to calculate continuous symmetry measures from atomic coordinates.‡

The present methodology offers two different options: to determine the *symmetry content* by searching for the nearest specific structure that belongs to the desired symmetry group (CSM), or to determine a *shape* or *form content*, that is the, distance to a pre-determined ideal structure (abbreviated CFM for *continuous form measure*). The idea of a polyhedral shape measure was earlier proposed by Dollase.[21] The ideal structure need not be symmetric at all and, from that point of view, eqn. (1) is a general shape measure. Both applications are of use and will be demonstrated below. In the case of the octahedron, form and symmetry measures coincide, since any octahedron has O_h symmetry. In the case of the trigonal prism, however, there are infinite choices of polyhedra with D_{3h} symmetry, depending on the choice of edges of the rectangular faces. We choose as the ideal polyhedron a trigonal prism with all its 9 edges of the same length, thus having two equilateral triangles and three squares as faces. This is not only the common geometric definition of a semiregular polyhedron,[22] but it is justified as the ideal trigonal prism from the chemical point of view since in the crystal structures of the different families of hexacoordinated compounds analyzed in this work, the vertical and horizontal edges (v and h in Fig. 1, respectively) of the coordination polyhedron are found to be roughly equal (*e.g.*, $0.97 \leqslant h/v \leqslant 1.10$ for hexamethyl complexes). In this case we determine not $S(D_{3h})$ but S(ideal trigonal prism), or S(itp). Of course, the symmetry of the nearest structure that is an equilateral trigonal prism is D_{3h} as well, and in general $S(D_{3h}) \leqslant S$(itp). Strictly speaking, $S(O_h)$ is a symmetry measure whereas S(itp) is a form measure, but we will refer to both within this paper as *symmetry measures* for simplicity.

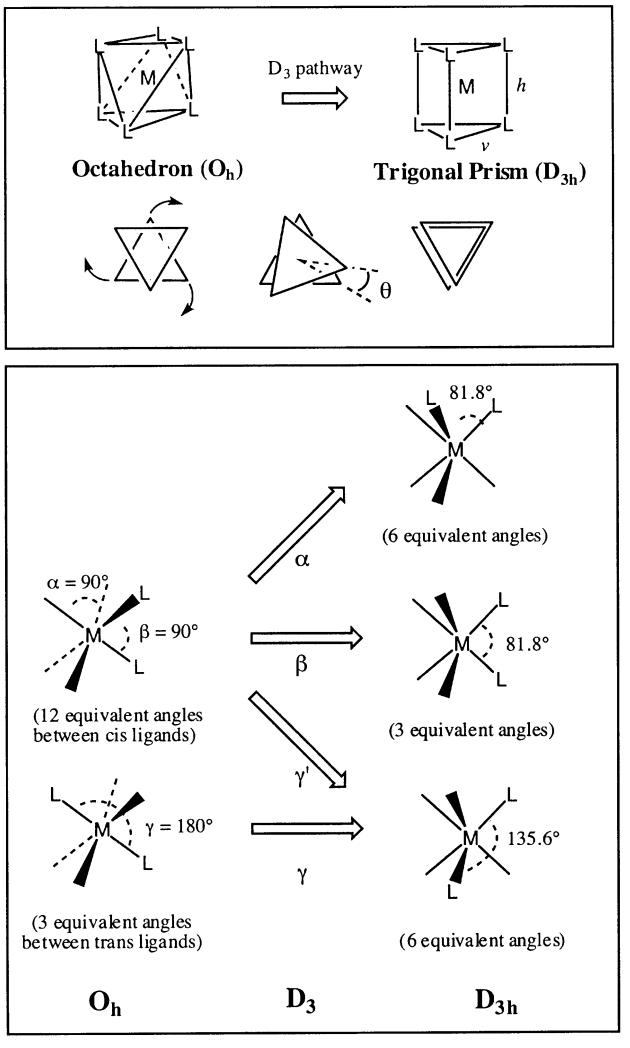

Fig. 1 Schematic description of the Bailar trigonal twist for the interconversion between the octahedron and the trigonal prism in ML_6 complexes (above) and of changes in the bond angles along the distortion pathway (below).

‡ Readers interested in testing and using our programs are encouraged to contact us at david@chem.ch.huji.ac.il.

Symmetry maps: molecular models of hexacoordinated polyhedra

We start our quantitative symmetry analysis of the structures of hexacoordinate transition metal compounds by studying the Bailar twist that interconverts the octahedron and the trigonal prism. Such a pathway connects two symmetry groups (O_h and D_{3h}) that do not have a group-subgroup relationship, passing through intermediate geometries belonging to the common subgroup D_3. We have previously explored the group-subgroup relationship for the case of the tetragonal distortion of the octahedron typically associated with a Jahn–Teller effect[23] and will discuss here the different behavior of the symmetry and shape measures in the two cases. These ideas will be extended to map the geometries of a variety of hexacoordinated complexes that include distortions of the two ideal polyhedra, and show that each distortion is represented by a specific line in the two-dimensional space defined by the two symmetry measures $S(O_h)$ and S(itp), a *symmetry map* for hexacoordination. Structures that present two or more simultaneous distortions may appear out of the studied tracks of the symmetry map, and we have analyzed the combined effect of the Bailar and Jahn–Teller distortions, both for a molecular model and for experimental structures, as well as the presence of these two distortions combined with trigonal distortions favored by facial tridentate ligands.

The Bailar twist

The most characteristic distortion of octahedral/prism systems is the Bailar trigonal twist,[11] leading from perfect O_h to perfect D_{3h} (including the itp). As shown in Fig. 1, the L–M–L bond angles (α, β, γ and γ') are different in the two ideal polyhedra, and they have been smoothly varied in our model along with the twist angle θ. The appropriate coordinate for such a distortion is the dihedral twist angle θ. For twist angles of 0, 120 and 240° we have perfect trigonal prisms, whereas for angles of 60, 180 and 270° we have perfect octahedra. In general it suffices to consider only the range between 0 and 60°. Structures with intermediate twist angles belong to the D_3 symmetry point group and are usually called *trigonal metaprisms*.[24] In Fig. 2 we show how S(itp) and $S(O_h)$ vary with the twist angle along such a pathway. It is seen that the extremes are at $n{\cdot}60°$ ($n = 0$, 1, 2, 3), and that even a perfect D_{3h} prism is characterized by residual octahedricity, represented by a high value of $S(O_h) = 16.73$. Conversely, the perfect octahedron is characterized by the *same* value of residual content of the prism, S(itp) = 16.73. The intermediate geometry with $\theta = 30°$ is isosymmetric with respect to the octahedron and the trigonal prism and has $S(O_h) = S$(itp) = 4.42. Thus, any structure that has $S(O_h) < 4.42$ [or S(itp) > 4.42] is closer to the octahedron than to the trigonal prism and can be best described as a *distorted octahedron*. Conversely, structures with $S(O_h) > 4.42$ [or S(itp) < 4.42] should be termed *distorted trigonal prisms*.

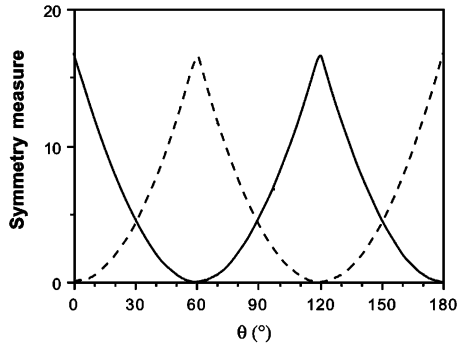

Fig. 2 Minimum distance to the O_h symmetry (continuous line) and to the ideal trigonal prism (dashed line) along the Bailar path for a model ML_6 complex.

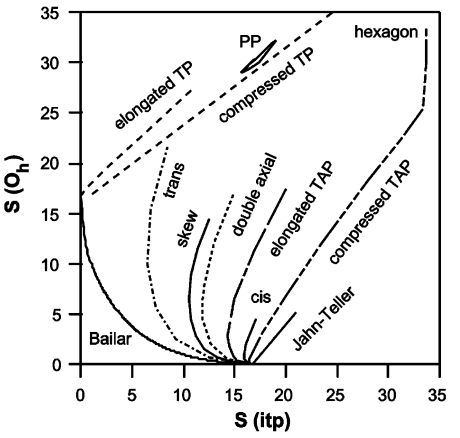

Fig. 3 Scatterplot of the octahedral and trigonal prismatic measures of a model ML_6 complex for several distortion modes: D_3 Bailar twist (Fig. 1, continuous curve); D_{3d} trigonal antiprism (**6**, compressed for $\alpha > 90°$, elongated for $\alpha > 90°$); C_{2v} skew trapezoidal (**9**); D_{2h} cis equatorial bending (**3**); D_{4h} Jahn–Teller distortion (**1**, rightmost continuous line); D_{2h} rhombic (**2**); D_{3h} trigonal prisms (**7**, compressed for $\alpha = 90°$, elongated for $\alpha > 90°$) and several pentagonal pyramids (PP) with C_{5v} symmetry.

The dependence of the octahedral symmetry measure with the twist angle can be approximately fitted to the following parabola for rotation angles θ between 0 and 120° (13 points, regression coeficient $r^2 = 0.999$):

$$S(O_h) = 16.98 - 0.558{\cdot}\theta + 4.653 \times 10^{-3}{\cdot}\theta^2 \qquad (2)$$

which reproduces the actual values to within 0.2 units.

The dependence of both $S(O_h)$ and S(itp) on the twist angle implies that a correlation must exist between the two symmetry measures. Indeed, a scatterplot of $S(O_h)$ as a function of S(itp) for several twist angles (Fig. 3, curve in the lower left corner) nicely shows such a correlation. The empirical correlation between the two symmetry measures can be expressed by eqn. (3) [the r.m.s. deviation of the calculated model values from eqn. (3) is 0.08 for 28 geometries along the Bailar path]:

$$\sqrt{S(O_h)} + \sqrt{S(\text{itp})} = 4.16 \qquad (3)$$

The observation represented by eqn. (3) is remarkable: It tells us that the purely Bailar-twist route is characterized by a unique characterisitc value; we therefore term the constant 4.16 as the *Bailar-twist symmetry constant*. Thus, if the sum of the square roots of the two symmetry measures differs from 4.2, this would indicate some non-Bailar behavior, and if the deviation from that symmetry content is significant this would indicate the coexistence of a distortion other than the Bailar twist (our analysis of experimental data below suggests that values higher than 4.6 are indicative of significant deviations from the Bailar pathway). An additional observation is that the distance between an octahedric AB_6 molecule and a trigonal prismatic one with the same A–B distance is 4.09. The symmetry constant is somewhat smaller than this value because the A–B distances in the itp closest to a given octahedron are slightly larger.

We note that the correlation between tetrahedricity and square planarity for tetracoordinated molecules that was previously fitted to an exponential[25] can be expressed[26] in a similar way, but with a different symmetry constant:

$$\sqrt{S(T_d)} + \sqrt{S(D_{4h})} = 5.92 \qquad (4)$$

Comparison of the two symmetry constants tells us that the square/tetrahedron distortion route requires larger atomic displacements than the octahedral/itp Bailar path. A detailed analysis of eqn. (4) will be reported elsewhere.

A twist of the octahedron by an angle θ can be represented by the atomic displacement vectors shown in Fig. 1, corresponding to a normal mode T_{2u} in the O_h point group. In the D_{3h} group, the same mode belongs to the A_1'' representation. Since there is no other mode of the same representation at the two extreme symmetries, the minimum displacement coordinates $|Q_k - P_k|$ [eqn. (1)] that can restore either symmetric shape corresponds precisely to the T_{2u} or A_1'' modes, which are identical except for the sign. A similar behavior has been found in the square-planar to tetrahedral interconversion pathway.[25] In contrast, the different numerical values that we found for the different bond lengthening distortions of the trigonal bipyramid[14] are associated with the existence of more than one mode of the same symmetry.

Now that we have seen that the Bailar pathway for the octahedron-trigonal prism interconversion is represented by a line in the two dimensional space of these two symmetry measures, we should ask ourselves where will a molecule with a different type of distortion from either the octahedron or the trigonal prism appear. Since every distortion of the two ideal polyhedra will be represented by a line in the $\{S(\text{itp}), S(O_h)\}$ space, we will build a map of the different distortion modes by plotting such pairs of values obtained along each particular distortion mode. Let us analyze then the behavior of these two symmetry measures for several distortions of a model hexacoordinated molecule.

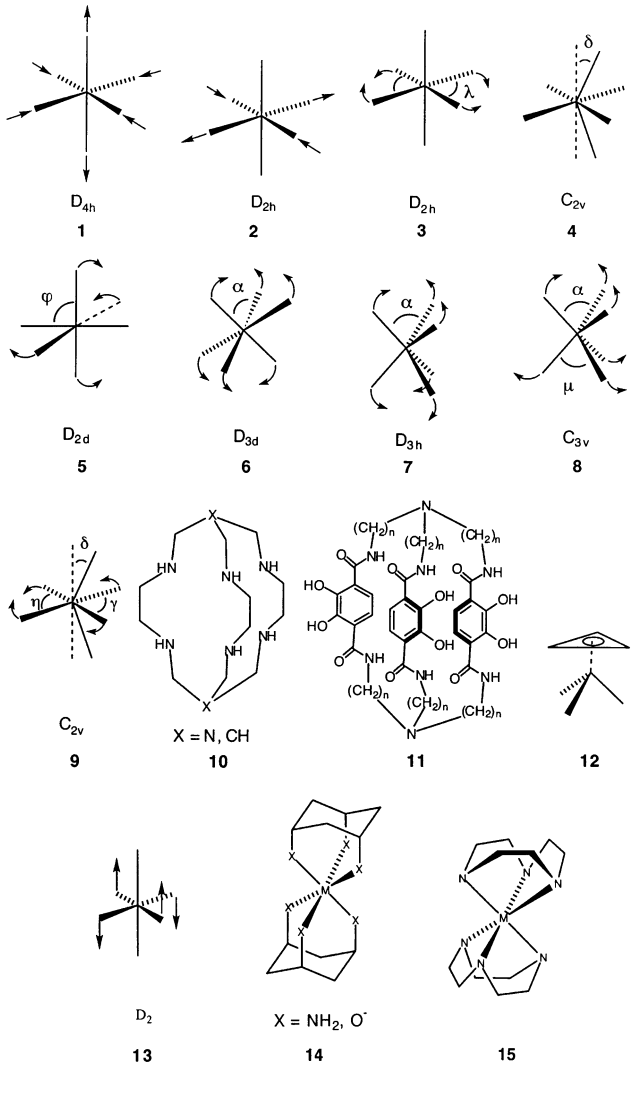

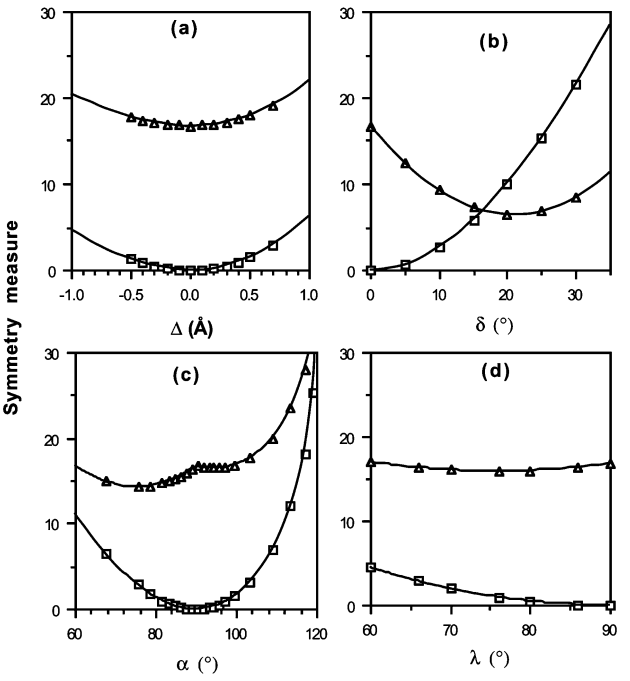

Fig. 4 Dependence of the $S(\text{itp})$ and $S(O_h)$ symmetry measures (triangles and squares, respectively) upon distortion of the octahedron through variation of different structural parameters: (a) the Jahn–Teller distortion **1** (Δ is the difference between axial and equatorial bond distances), (b) the skew-trapezoidal distortion **9** (δ, η and γ varied simultaneously), (c) the elongated ($\alpha < 90°$) and compressed ($\alpha > 90°$) trigonal prisms (**7**) and (d) the equatorial bending distortion **3**.

Jahn–Teller tetragonal distortion

This distortion (**1**) has been previously discussed with regard to the octahedral symmetry measure.[23] We calibrate here the degree of tetragonal distortion by the difference between long and short bond distances, Δ, adopting a positive sign for elongated octahedra (*i.e.*, two long and four short bond distances) and a negative sign for the opposite distortion leading to compressed octahedra. The dependence of the two symmetry measures on Δ is shown in Fig. 4(a): both increase upon departure from the octahedron. The dependence of the octahedral symmetry measure with the distortion parameter can be fitted (regression coefficient $r^2 = 1.000$ for 7 points) to the following expression:

$$S(O_h) = 5.39 \cdot \Delta^2 - 0.33 \cdot | \Delta | \qquad (5)$$

In the symmetry map (Fig. 3), the tetragonal distortion is represented by a straight line [eqn. (6) regression coefficient $r^2 = 0.996$ for 7 points]:

$$S(O_h) = 1.23\ S(\text{itp}) - 20.52 \qquad (6)$$

that is clearly differentiated from other distortions of the octahedron analyzed below. We note that the same line is obtained regardless of the metal-ligand distance chosen for the undistorted octahedron, indicating its generality and the global nature of the symmetry measure (we have used 2.0 and 2.2 Å for our molecular model).

We note that compressed and elongated octahedra fall along the same line of the symmetry map, and also that the Jahn–Teller line of the symmetry map seems to represent the upper limit for $S(\text{itp})$ at a given $S(O_h)$ value.

Combined effect of Jahn–Teller and Bailar distortions of the octahedron

One can imagine a bond stretch Jahn–Teller distortion acting on a twisted octahedron. Symmetry measure calculations on

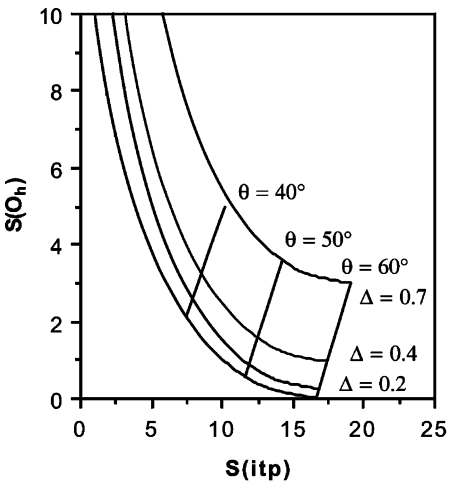

Fig. 5 Effect of a Jahn–Teller distortion upon the symmetry measures of an hexacoordinated model molecule with different twist angles θ (straight lines). The bottom curve represents the Bailar twist with all metal–ligand bond distances equal.

a model with such a combination of the two distortions show a dependence on Δ [Fig. 5 and eqns. (7) and (8) for twist angles of 50 and 40°, respectively] similar to that found for a Jahn–Teller distortion from the perfect octahedron [$\theta = 60°$, eqn. (5)], the main difference being the independent term that corresponds to the values of the pure Bailar twist (Fig. 2). The relationship between the octahedricity and the trigonal prismacity for *Jahn–Teller* distortions of twisted octahedra is represented by straight lines practically parallel to that of the tetragonal distortion from a perfect octahedron [Fig. 4(b)] and can be expressed by eqns. (9) and (10) for twist angles of 50 and 40°, respectively.

$$\theta = 50°\text{: } S(O_h) = 0.53 + 6.258 \cdot \Delta^2 - 0.172 \cdot \Delta \quad (7)$$

$$\theta = 40°\text{: } S(O_h) = 2.08 + 6.118 \cdot \Delta^2 - 0.167 \cdot \Delta \quad (8)$$

$$\theta = 50°\text{: } S(O_h) = 1.07 \cdot S(\text{itp}) - 6.00 \quad (9)$$

$$\theta = 40°\text{: } S(O_h) = 1.14 \cdot S(\text{itp}) - 12.90 \quad (10)$$

The present results indicate that the Bailar curve in the symmetry map of Fig. 3 represents the maximum octahedricity [*i.e.*, the minimum $S(O_h)$ value] for a given S(itp) or for a given twist angle.

Rhombic distortion

A rhombic distortion can be produced by stretching two and simultaneously shortening two other trans bond distances while keeping all bond angles constant at 90° (**2**). The resulting D_{2h} symmetry point group is a different subgroup of O_h than that corresponding to the rectangular bipyramid produced upon an equatorial bending distortion, since the σ_v symmetry planes preserved are those containing the M–L basal bonds in the rectangular bipyramid, but the ones bisecting those bonds are preserved in the rhombic bipyramid. Such distortion has an effect on the octahedral and trigonal prismatic measures very similar to the simpler tetragonal distortion discussed above: both symmetry measures increase upon distortion. If we measure the degree of distortion by the difference between the longest and shortest distances (Δ), the dependence of the symmetry measures on Δ is quite similar to that in a tetragonal distortion. The correlation between the two measures is practically identical (with a deviation of at most 0.04 units) to that found for the tetragonal distortion [eqn. (6)], and the distance to the perfect octahedron for even a large distortion (*e.g.*, $\Delta = 0.8$ Å) is relatively small (2.60) compared to those of the angularly distorted structures analyzed in this work.

Equatorial bending

Changes in the equatorial bond angles of the octahedron (**3**) while keeping the bond distances constant result in rectangular bipyramids with D_{2h} symmetry. The changes in the symmetry measures are represented as a function of the bond angle λ in Fig. 4(d). As could be expected, such distortion produces an increase in $S(O_h)$ but the distance to the ideal trigonal prism, S(itp), is little affected. The result is a line on the symmetry map in-between those of the elongated and compressed trigonal prisms (labelled cis in Fig. 3). An analysis of the sum of the square roots of the two symmetry measures indicates that it increases linearly as the bond angle deviates from 90°, in agreement with our above interpretation that such a parameter adopts the value 4.2 for structures that experience only a Bailar twist, but larger values for structures that present other types of distortions.

Axial bending

Tilting two axial ligands (**4**) distorts the octahedron to the C_{2v} symmetry subgroup. The tilt angle δ has been varied from 0 to 30° and it is seen to affect more significantly the octahedricity than the trigonal prismacity. The relationship between $S(O_h)$ and S(itp) is an interesting curled line in the symmetry map (Fig. 3, curve labeled trans). The curled line means that two structures with different degrees of distortion from the octahedron [*i.e.*, with different $S(O_h)$ values] are isosymmetric with respect to the ideal trigonal prism [*i.e.*, have the same S(itp) value]. At a deviation of 40° from the axial positions, the geometry of the molecule is equidistant to the octahedron and the trigonal prism. This and other distortions have in common that they initially deviate from the octahedron and seem to approach the trigonal prism, but they can never reach the trigonal prism upon further distortion, which is why the curves are bent back.

Double axial bending

If two sets of trans ligands are distorted in such a way (**5**) that the corresponding trans L–M–L bond angles are less than 180°, the symmetry of the molecule lowers to D_{2d}. The degree of distortion can be measured by the cis angles that are 90° in the perfect octahedron and decrease as the distortion proceeds. Such distortion is in practice found when *mer*-spanning tridentate ligands such as terpyridine are used, but also in a variety of minerals as will be shown elsewhere.

The trigonal antiprism and the hexagon

If the six bond angles α of the octahedron (Fig. 1) are made smaller than 90°, an elongated trigonal antiprism of D_{3d} symmetry results (**6**). Conversely, angles larger than 90° produce a compressed trigonal antiprism that belongs to the same symmetry group. Both elongation and compression of the octahedron along a trigonal axis produce an increase in the $S(O_h)$ value [Fig. 4(c), squares]. However, S(itp) behaves in different ways for compression and elongation [Fig. 4(c), triangles]. In the first case ($\alpha > 90°$), S(itp) is practically unaffected by small distortions, but increases with the angle if α is greater than 105°. For an elongated trigonal antiprism, though, S(itp) decreases and then increases upon decreasing α. When these results are incorporated into the symmetry map (Fig. 3), two distinct lines result: one for the elongated and one for the compressed trigonal antiprism (TAP). We can conclude that S(itp) must be larger than 14 for elongated and larger than 17 for compressed trigonal antiprisms.

Taking the axial compression of an octahedron to the extreme would lead to a hexagon. Therefore, the position of the hexagon in the symmetry map is at the end of the line corresponding to the compressed trigonal antiprism. Interestingly, the hexagon is at nearly the same distance from the octahedron as from the trigonal prism, as reveal the symmetry measures calculated for a model hexacoordinated molecule: $S(O_h) = 33.33$ and $S(\text{itp}) = 33.68$, in the upper right corner of the symmetry map (Fig. 3).

Compression and elongation of the trigonal prism

Simultaneous changes in the six bond angles α (Fig. 1) of the trigonal prism, as in **7**, retain the D_{3h} symmetry. Angles of less than 81.8° correspond to elongated trigonal prisms with $v > h$, and larger angles to compressed trigonal prisms with $v < h$. In both cases S(itp) increases because the reference shape (the itp) is that with $h = v$. $S(O_h)$ increases both upon elongation and compression of the trigonal prism. Consequently, these distortions appear in a specific region of the symmetry map (Fig. 3) as two neighboring lines [that can be approximated to linear eqns. (11) and (12) for compressed and elongated trigonal prisms, respectively, with regression coeficients r^2 of 0.998 in both cases]:

$$S(O_h) = 0.75\ S(\text{itp}) + 16.40 \quad (11)$$

$$S(O_h) = 0.97\ S(\text{itp}) + 16.88 \quad (12)$$

The most elongated trigonal prism we have tried is one with $\alpha = 51°$ ($v/h = 2.00$) and appears at {10.7, 27.2}. On the other hand, the most compressed trigonal prism in Fig. 3 is a hypothetical one in which the two triangular faces have collapsed into one triangle, and its symmetry measures correspond to the {42.9, 50.0} point on the symmetry map.

Truncated trigonal pyramid (C_{3v} distortion of the trigonal prism)

If the three upper α angles of a trigonal prism are decreased from those of the ideal polyhedron while the lower ones are increased (**8**), a truncated trigonal pyramid of C_{3v} symmetry results. Such distortion takes us away from the trigonal prism and from the octahedron as well, and is represented by a straight line in the symmetry map (not shown in Fig. 3), indicating that such a distortion increases equally the distance to the octahedron and to the trigonal prism. This line is practically coincident with that of a compressed trigonal prism, and can be represented by the least-squares equation:

$$S(O_h) = 0.59\ S(\text{itp}) + 16.74 \quad (13)$$

Skew-trapezoidal bipyramid

If the axial bending discussed above is combined with a distortion of the equatorial ligands to a trapezoid (**9**), a skew-trapezoidal bipyramid with C_{2v} symmetry is formed. The dependence of the octahedral and trigonal prismatic measures as a function of such distortion is presented in Fig. 4(b). An interesting situation appears at $\delta \approx 16°$, since the distorted structure is isosymmetric with respect to the octahedron and the trigonal prism.

The pentagonal pyramid

A pentagonal pyramid is characterized by C_{5v} symmetry, but is not uniquely defined. With that symmetry, the axial and equatorial bond lengths are independent and one can conceive an infinite number of pyramids characterized by different axial/equatorial ratios. On the other hand, the central atom needs not be coplanar with the five basal ligands and again different pyramids exist for a given bond distance ratio depending on the L_{ax}–M–L_{eq} bond angle. We have varied these two parameters for a model pentagonal pyramid ML_6 complex ($0.77 \leqslant$ axial/equatorial ratio $\leqslant 1.46$ and $90° \leqslant L_{ax}$–M–$L_{eq} \leqslant 120°$) and the corresponding symmetry measures are plotted on the symmetry map (Fig. 3).

Although the actual symmetry measures for a given pyramid vary with the two structural parameters just mentioned, all the values appear between the {16, 29} and {19, 32} points. These are roughly represented by the following linear equation for $S(\text{itp}) > 15$:

$$S(O_h) = S(\text{itp}) + 13.29 \quad (14)$$

We have not modeled the transformations from a pentagonal pyramid to an octahedron or a trigonal prism, but it is obvious that any sensible pathway for those transformations should connect these points with {16.7, 0} and {0, 16.7}, respectively.

Symmetry map and rules for shape classification

According to the analysis of the structures of model molecules, the structure of every hexacoordinated polyhedron can be identified by its position on the symmetry map presented in Fig. 3, given by the pair of coordinates {S(itp), $S(O_h)$}. From such coordinates, a good qualitative description of the structure can be obtained in many cases.

Rule (1) Structures represented by the {16.7, 0} point on the symmetry map correspond to perfect octahedra.

Rule (2) Structures at point {0, 16.7} on the symmetry map correspond to ideal trigonal prisms.

Rule (3) Other values that obey eqn. (3) correspond to metaprisms along the Bailar path that connects the octahedron and the trigonal prism. According to the distance criterion of eqn. (3), structures with $S(O_h) < 4.42$ [or $S(\text{itp}) > 4.42$] are closer to the octahedron than to the TP and are best described as twisted octahedra. Conversely, structures with $S(O_h) > 4.42$ [or $S(\text{itp}) < 4.42$] are best described as twisted trigonal prisms.

Rule (4) Molecular structures with a pair of symmetry measures that do not obey the sum rule of eqn. (3) (*i.e.*, the sum of square roots is significantly greater than 4.2) correspond to structures that present some distortion other than the Bailar twist, or even the coexistence of a Bailar twist and another distortion. We have found that significant distortions give square root sums larger than 4.6.

Rule (5) A tetragonal bipyramid characteristic of pure Jahn–Teller distortions of the octahedron is indicated by an S(itp) value larger than 17 and its $S(O_h)$ value should obey eqn. (5).

Rule (6) The simultaneous presence of Bailar and Jahn–Teller distortions is characterized by a square root sum of 4.6 or higher, and the position of such a distorted structure on the symmetry map is illustrated by eqns. 7 and 8 and Fig. 5, depending on the angular and distance parameters θ and Δ.

Rule (7) Values close to the line represented by eqn. (11) may correspond to compressed trigonal prisms. The elongated trigonal prisms can be found in a nearby region of the symmetry map, with symmetry measures corresponding to the approximate eqn. (12). Trigonal prisms distorted towards a truncated trigonal pyramid (C_{3v} symmetry) appear in a similar region of the symmetry map, approximated by eqn. (13). Although the presence of a distortion of the trigonal prism that retains the trigonal rotation and the σ_v reflections of the D_{3h} group can be easily identified by their position on the symmetry map at values of S(itp) larger than 17 and relatively small values of $S(O_h)$, these three types of distortions cannot be reliably differentiated from each other from the numerical values of their symmetry measures only.

Rule (8) The set of coordinates {35, 35} corresponds to a regular hexagon. Deviations of a few units of either symmetry measure indicate puckered rings.

Rule (9) Symmetry measures near those of the compressed or elongated trigonal prisms, between {15, 28} and {19, 32},

can in principle be attributed to a pentagonal pyramid. The two types of structures can be discriminated by analyzing the $S(C_5)$ and $S(C_3)$ symmetry measures.

Analysis of experimental data

A. Hexakis(monodentate) complexes

We have taken as a reference set the structures of the homoleptic complexes with thiolato, alkyl or aryl ligands. Other families of homoleptic hexacoordinated complexes with monodentate ligands have been analyzed, but will not be discussed here since all structures are either practically octahedral (*i.e.*, $\theta \approx 60°$) or Jahn–Teller distorted: $[MX_6]^{n-}$ (X = halide), $[M(NR_2)_6]^{n-}$, $[M(OR)_6]^{n-}$, $[M(SCN)_6]^{n-}$, $[M(CO)_6]$, $[M(CN)_6]^{n-}$. The analysis of the structural parameters of the reference set of compounds allows us to draw the following conclusions.

(1) These families present examples of a variety of structures from octahedral to trigonal prismatic, as indicated by their twist angles θ (structural data and symmetry measures provided as Electronic supplementary information).

(2) The angular parameters behave as expected from the geometric description of Fig. 1. Hence, the angles α and β decrease upon rotation from octahedron to trigonal prism, even if the values of β are slightly smaller (by some 3°) than those of α when approaching the trigonal prism. The angles γ in the approximately trigonal prismatic structures have average values close to 136°.

(3) Good correlations are found between the different angular parameters (α, β, γ or θ) and the vertical normalized bite $b_v = v/d$, where d is the average metal-to-ligand bond distance and v is the length of the edges that join the two trigonal faces (see Fig. 1). Note that although the term *bite* applies to bidentate ligands, we retain it here to denote the edges that would be occupied by chelating ligands even when we are looking at complexes with monodentate ligands. The values of d associated with the variety of metal atoms considered are not correlated with these parameters. This result indicates that the bond angles and the normalized bite are essentially governed by the twist angle. It is interesting to note that a correlation between the bite and twist angle was reported by Kepert[27] for tris(chelate) complexes, but has been so far attributed to the bidentate nature of the ligands in those compounds, whereas we find here that such a correlation exists also for complexes with monodentate ligands and appears to be a geometrical characteristic intrinsic to the Bailar route that links the octahedron and the trigonal prism.

(4) The vertical normalized bites of hexamethyl complexes clearly decrease from the octahedron ($1.37 < b_v < 1.43$) to the trigonal prism ($1.23 < b_v < 1.28$), following the geometrical expectations for the ideal trigonal twist (ideal bite angles for the octahedron and the trigonal prism are 1.41 and 1.31, respectively). The *horizontal* normalized bite ($b_h = h/d$, Fig. 1), in contrast, changes less along the same path ($1.35 < b_h < 1.46$ for octahedral, $1.33 < b_h < 1.36$ for trigonal prismatic structures). The latter result is probably due to the C_{3v} distortion of the trigonal prism commented above.

(5) These structures adapt well to our choice of the ideal trigonal prism in which horizontal and vertical edges are identical (square faces), since these two edges in a particular compound are roughly equal (*e.g.*, $0.97 \leqslant h/v \leqslant 1.10$ for hexamethyl compounds).

(6) All those structures that are significantly twisted from the octahedron ($\theta < 40°$) correspond to metal ions with d^0 to d^2 electron configurations, whereas all complexes with d^3 to d^{10} configurations are characterized by $\theta \geqslant 40°$. Among the family of organometallic compounds, all d^0 and d^1 complexes are approximately trigonal prismatic, except for

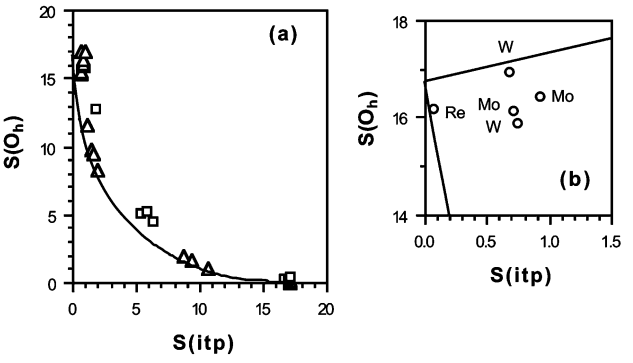

Fig. 6 (a) Scatterplot of the octahedron and trigonal prism symmetry measures of homoleptic complexes with monodentate ligands as a function of the twist angle θ. Triangles correspond to organometallic, squares to thiolato complexes. (b) Blow-up of the trigonal prismatic region of the symmetry map showing the experimental data of $[MMe_6]$ complexes that are significantly distorted from the ideal trigonal prism.

$[M(C{\equiv}CSi\{^tBu\}_3)_6]$ (M = Zr, Hf), in which the bulky alkynyl ligands are probably responsible for the adoption of an octahedral geometry that has a larger bite (*i.e.*, longer Bu···Bu contacts). No clear geometric preference is found for thiolato d^0 and d^1 complexes, the twist angles in this family varying between 9 and 60°.

Having seen that the reference set of homoleptic complexes with monodentate ligands provides a wide sample of geometries between octahedral and trigonal prismatic and that other angular parameters are correlated to the twist angle, we can now analyze the behavior of the continuous symmetry measures relative to the two ideal polyhedra along the trigonal twist pathway by looking at their position on the symmetry map (Fig. 6). The experimental structures analyzed are nicely aligned along the Bailar pathway, a fact that is numerically reflected by their square root sums (rule 3) of less than 4.6 in most cases. The molecules that deviate significantly from the Bailar pathway (rule 4) are those at the upper left end of the symmetry map and correspond to the different crystallographically independent molecules of $[MoMe_6]$ and $[WMe_6]$. The behavior of such molecules can be better seen in a blow-up of the symmetry map [Fig. 6(b)]. Two such molecules appear clearly along the C_{3v} path while the others seem to present that distortion combined with a small Bailar twist. The existence of such distortions is corroborated by a detailed analysis of the bond angles (differences in bond angles at the two MMe_3 groups of each molecule are of about 19°). The analogous Re compound, twisted by only one degree from the trigonal prism but with no C_{3v} distortion, is slightly shifted downward along the Bailar curve and is shown in Fig. 6(b) for reference.

B. Trischelate complexes

To analyze the effect of the presence of chelate rings on the choice between the octahedron and the trigonal prism, we have analyzed the structures of a variety of [M(bidentate)$_3$] complexes, where bidentate represents dithiolene, diselenolene, dithiocarbamate, ethylenediamine, β-diketonate or bipyridine (433 crystallographically independent molecules from 325 chemical compounds). For other ligands (carboxylates, amidinates and diarsines), a small number of structures were found and these will not be discussed here. When studying complexes with bidentate ligands the important edges are those occupied by the chelating groups, hence, according to our convention of orienting the trigonal axis vertically (Fig. 1), we will be concerned only with the *vertical* normalized bite b_v

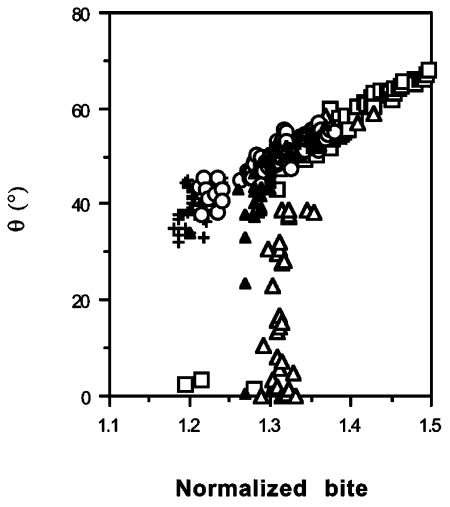

Fig. 7 Trigonal twist angle in several families of tris(bidentate) complexes as a function of the normalized bite. Squares correspond to β-diketonates, triangles to dithiolenes and diselenolenes, crosses to dithiocarbamates, open circles to ethylenediamine and closed circles to metal chalcogenides with MX_2 stoichiometry.

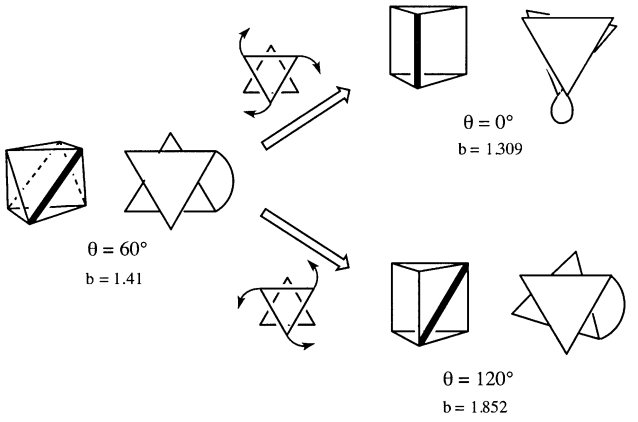

Fig. 8 Schematic representation of the different disposition of a bidentate ligand in a trigonal prism that is obtained by a clockwise (above) or an anticlockwise (below) trigonal twist by an angle θ. The two vertices occupied by the bidentate ligand are joined by a thick line in the perspective representations, and the bidentate ligands are represented by arcs in the projections. The normalized bite (b) that corresponds to the ideal polyhedron in each case is also given.

throughout this section and will refer to it simply as the normalized bite, thus omitting the subscript.

A scatterplot of the twist angle as a function of the normalized bite for all complexes studied clearly shows the coexistence of two different trends (Fig. 7). Besides the simple linear dependence between the normalized bite and the twist angle reported by Kepert,[27] one can see a group of structures with similar normalized bites of around 1.3 but having a variety of twist angles between 0 and 45°. Hence, for the latter compounds there is no correlation between b and θ. To better understand the two alternative trends observed it is worth discussing separately the different families of compounds classified by ligands.

For dithiolenes, diselenolenes and β-diketonates the normalized bite and the twist angle correlate approximately in the same way as for the monodentate ligands (see previous section). Thus, the normalized bite for octahedral complexes ($\theta \approx 60°$) is close to 1.4, and tends to values of around 1.3 for trigonal prismatic molecules ($\theta \approx 0°$). There seems to be a clear correlation between electron configuration and geometry in dithiolene and diselenolene complexes. Hence, all such compounds with d^0 to d^2 electron configurations are severely twisted toward the trigonal prism ($\theta < 40°$), one d^3 compound has $\theta \approx 40°$ and two cases identified with a d^6 configuration have $\theta \approx 60°$.

Among the β-diketonates, most of the complexes are approximately octahedral, including three cases with d^0 or d^1 configuration, although all trigonal prismatic structures correspond to d^0 ions. It is interesting to note that the β-diketonato complexes present twist angles larger than 60°. If we focus on the edges occupied by bidentate ligands in molecular structures intermediate between octahedral and trigonal prismatic (Fig. 8), we can see that three edges of the octahedron are converted to vertical edges of the trigonal prism, whereas the other three are converted into diagonals of the square faces. For chelating ligands two cases can be distinguished: (*i*) a clockwise twist (from $\theta = 60°$ to $\theta = 0°$) leads to a trigonal prism with the bidentate ligand occupying a vertical edge; and (*ii*) an anticlockwise twist (from $\theta = 60°$ to $\theta = 120°$) results in a trigonal prism with the chelate ring occupying the diagonal of a square face. In contrast, in complexes with all monodentate ligands, the clockwise and anticlockwise twists are equivalent. Since the normalized bite b_v decreases from the octahedron to the trigonal prism in the clockwise twist but increases with an anticlockwise twist, one should expect the clockwise twist to appear for complexes with small normalized bite, and the anticlockwise twist for those with large normalized bites. Among the bidentate ligands analyzed here, the dithiocarbamates show the smallest normalized bite (1.21 for first row transition metals) and the β-diketonates the largest one (1.41), therefore explaining the anticlockwise twist observed for the β-diketonates.

Complexes of ethylenediamine, bipyridine and dithiocarbamates present a linear dependence between θ and b, but none of these complexes is even close to the trigonal prism. In the ethylenediamine family, the twist angles are comprised between 38 and 57° for complexes with electron configurations from d^3 to d^{10}. The wider range of normalized bites and twist angles in the ethylenediamine family is associated with a large standard deviation in the donor–donor distances (0.10 Å) that reflects the flexibility of the N–C–C–N backbone, but also a good correlation is found between b and the M–L distance. In this family, the smallest b and θ values correspond to complexes of the Cd^{2+} and Mn^{2+} ions.

The dithiocarbamate complexes present electron configurations between d^2 and d^{10}, and their twist angles cluster at around 40°. The narrower distribution of θ and b values for dithiocarbamates is associated to the rigidity of the CS_2 core, substantiated by a small standard deviation of the S···S distance (0.05 Å).

A plot of the structural data for the tris(bidentate) complexes analyzed here in a symmetry map is presented in Fig. 9, where most of these structures are seen to be aligned along the Bailar pathway. The sum of the square roots of the two symmetry measures provides us some insight into the stereochemistries of these families of compounds, and its distribution is shown in Fig. 10. There it can be seen that most structures present values close to that expected for a pure Bailar twist (4.1), but complexes with bipyridine or dithiocarbamates present a distribution centered at higher values. This must be attributed to the significantly smaller bite angles presented by these bidentate ligands [78 (4) and 71° (4) for bipyridine and dithiocarbamates, respectively], as discussed above for the model equatorial bending distortion, and is reflected by their deviation from the model Bailar twist in the symmetry map (rule 4).

An interesting conclusion that stems from the present analysis is that a trigonal prismatic structure can be achieved only if (*i*) the metal has a d^0 to d^2 electron configuration and (*ii*) the

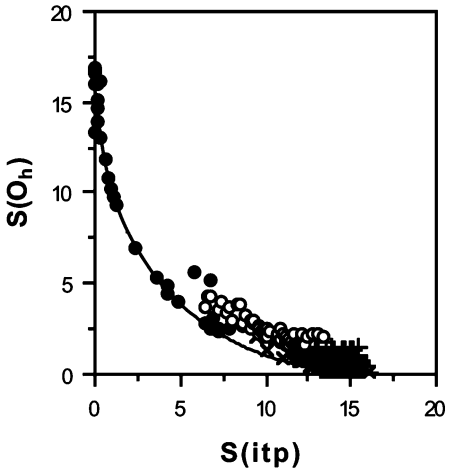

Fig. 9 Relationship between octahedral and trigonal prismatic symmetry measures for a variety of homoleptic hexacoordinate transition metal complexes with mono- or bidentate ligands. Data are shown for the following ligands: methyl or alkyl (open triangles), thiolates (open squares), ethylenediamine (crosses), bipyridine (plus signs), dithiocarbamates (open circles), and dithiolenes (closed circles). The solid line corresponds to the ideal path (Figs. 1 and 3).

normalized bite is smaller than 1.34. If either of the two conditions is not met, a twisted octahedron is preferred, with the twist angle determined by the normalized bite according to the approximate expression given in eqn. (15) (regression coefficient r^2 of 0.796 for 379 data sets):

$$\theta = 88.0b - 64.9 \qquad (15)$$

Of the compounds analyzed here, all those with electron configurations between d^3 and d^{10} show twist angles θ larger than 27°. The only three exceptions to these rules are a d^{10} $[Cd(acac)_3]^-$ anion[28] and two d^5 Fe(III) complexes with catecholato encapsulating ligands **11**.[29,30]

An illustration of this principle is provided by the structures of several early transition metal diketonates. V(IV), Ti(IV) and Sc(III) complexes with d^0 to d^2 configurations but with normalized bites of ~1.4 are nearly octahedral,[31–35] whereas the d^0 Y(III) analog[36,37] with a normalized bite of 1.2 is trigonal prismatic. It is interesting to note that extrapolation of eqn. (15) to $\theta = 0$ would predict that a trigonal prismatic structure might be reached for a normalized bite of 0.74, but the only bidentate ligand that can approach such a small bite is a side-on bonded peroxo anion (0.77 for first row, 0.75 for second and third row transition metals); the next smallest bites are those of the BH_4^- (0.98 and 0.95) and the triazenido (0.99 and 0.96) anions.

C. Complexes with encapsulating ligands

An encapsulating ligand can be described as formed by three bidentate ligands held together by chemical bonds. At first sight it seems that encapsulating ligands may impose additional restrictions on the bites of the three chelate rings formed upon coordination to a metal atom, with a corresponding effect on the geometry choice between octahedron and trigonal prism. To analyze the behavior of encapsulating ligands, we have looked at the families of complexes with ligands of the types depicted in **10** and **11**. The chelating groups have the ethylenediamine core in **10** and catecholato groups in **11** (conveniently deprotonated to form hexa-anions). The family of complexes with N-donor encapsulating ligands presents a variety of structures intermediate between the octahedron and the trigonal prism.[38] A scatterplot of the two symmetry measures in these complexes (Fig. 11) reveals Bailar deviations from the octahedral symmetry similar to those found for trischelate complexes with ligands such as ethylenediamine or diketonate. Similarly, several complexes of catecholato encapsulating ligands present varying degrees of distortion from the octahedral geometry (data and references provided as Electronic supplementary information). The values of the twist angle in these compounds show a sharp drop with decreasing normalized bite, just like the hexamethyl or tris(dithiolene) complexes discussed above, and those with nearly trigonal prismatic structures are d^0, d^1, or high-spin Fe(III) d^5 complexes. The octahedral and trigonal prismatic measures for these complexes nicely follow the general trend of eqn. (3) (Fig. 12).

D. Cu(II) complexes and Jahn–Teller distortion

To best appreciate the effect of the bond stretch Jahn–Teller distortions in Cu(II) complexes, we have selected the structures of those compounds in which the difference between the longest and shortest copper–ligand bond lengths (represented hereafter by Δ) is larger than 0.7 Å, and their pair of symmetry measures are represented in the symmetry map of Fig. 13. There one can observe that (*i*) many structures fall along the ideal Jahn–Teller path **6** discussed above for a theoretical model (rightmost straight line): 32 out of 227 structures present $S(O_h)$ values that deviate less than one unit from those expected for a pure Jahn–Teller distortion [rule 6, eqn. (6)];

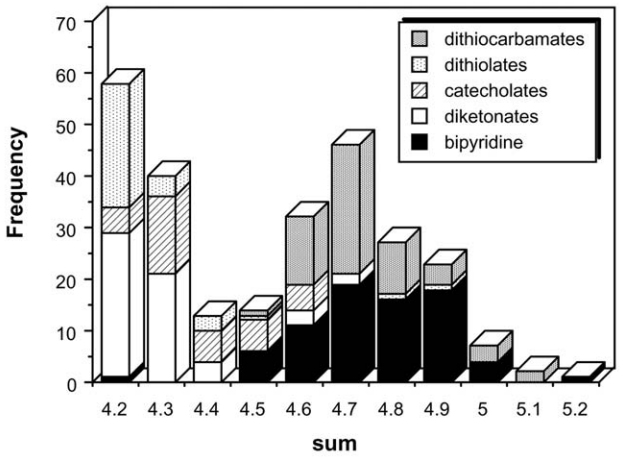

Fig. 10 Distribution of the sum of the square roots of $S(O_h)$ and S(itp) for several families of tris(chelate) complexes. The value expected for structures along the D_3 Bailar twist [eqn. (3)] is 4.16. The ethylenediamine complexes, not included in the histogram, appear concentrated at the extreme left.

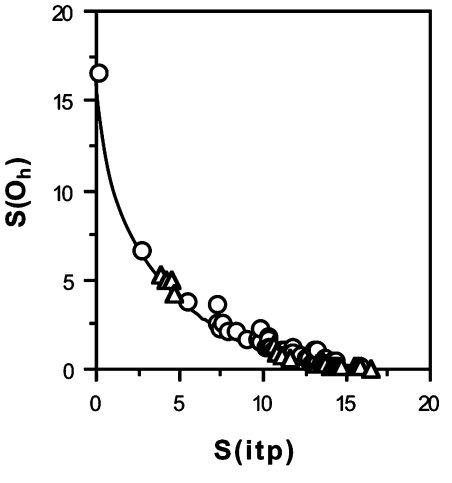

Fig. 11 Relationship between octahedral and trigonal prismatic symmetry measures for encapsulating hexaamine (**10**, squares) and tris(catecholato) (**11**, triangles) complexes.

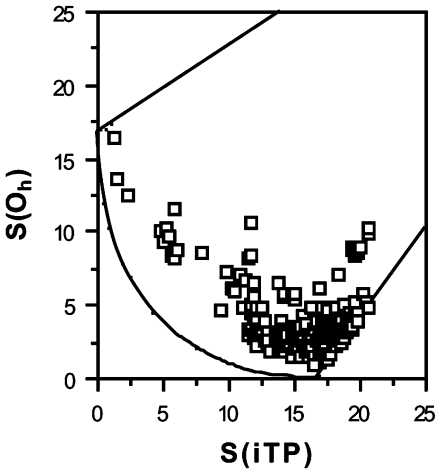

Fig. 12 Octahedral and trigonal prismatic symmetry measures for Cu(II) complexes with a difference between the longest and shortest metal–ligand bond lengths (Δ) larger than 0.7 Å. The straight lines represented correspond to the C_{3v} distortion of the trigonal prism (left) and the D_{4h} bond stretch distortion of the octahedron (right). The bottom curve corresponds to the Bailar twist with all metal–ligand distances equal.

(*ii*) none of the structures corresponds to the ideal Bailar path, since in all cases the bond stretch distortion is superimposed on the trigonal twist, as reflected in square root sums of 4.9 or higher; (*iii*) the effect of the Bailar and Jahn–Teller distortions on the symmetry measures is approximately additive, as found above for the molecular models; (*iv*) the Jahn–Teller line on the symmetry map marks the lowest $S(O_h)$ value for S(itp) > 17. It is interesting to discover in that plot three structures of nearly trigonal prismatic Cu(II) complexes [S(itp) < 3]. These correspond to molecules with tetradentate macrocyclic ligands that occupy a square face of the trigonal prism, while the two remaining coordination positions are occupied by pending pyridyl groups.[39–41] Even if one of the donor atoms of the macrocyclic ligands is at a long distance from the Cu atom, the values of S(itp) for these complexes unequivocally correspond to a *slightly distorted* trigonal prism.

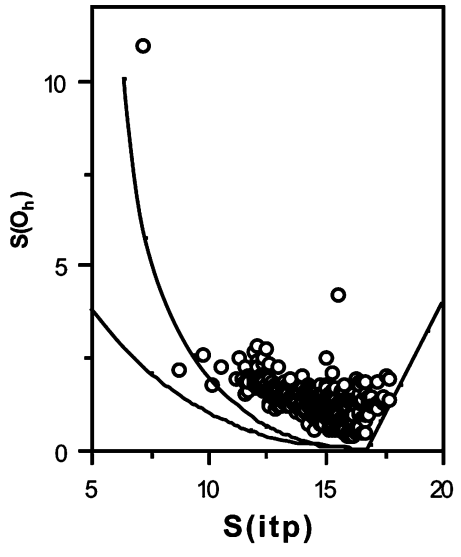

Fig. 13 Position of the experimental structures of *cis*-[MoO_2L_4] complexes (circles) on the symmetry map. The two continuous lines correspond (from bottom to top) to the Bailar twist and to the axial bending of two trans ligands (**4**).

E. cis-Dioxomolybdenum complexes

Molybdenum complexes with the general formula *cis*-[MoO_2L_4] are known to present a clear deviation of the two trans ligands L from the pseudotetragonal axis, showing L_{ax}–Mo–L_{ax} bond angles in the range between 138 and 170°. These compounds appear on the symmetry map (Fig. 13) along the line of the corresponding model distortion of the octahedron (**4**), clearly separated from the Bailar route as reflected by square root sums in excess of 4.6 (only three structures out of 483 data sets present values between 4.4 and 4.6). The hexacoordinated Mo atoms in a compound[42] with nuclearity 14 present bond angles as low as 110° and appear in Fig. 13 at {7.2, 11.0}, well separated from the rest of the structures, but in agreement with the expectations for the model curve. The ideal curve of the axial distortion **4** represents a lower limit for the position of these structures in the symmetry map (Fig. 13). There are two clear exceptions to the general behavior described by the model curve. One[43] corresponds to a compound in which bidentate ligands force deviations of the two axial donor atoms through planes that do not bisect the two Mo–O bonds as in **4** (*i.e.*, C_2 rather than C_{2v} symmetry) and appears at {8.7, 2.2}. The other exception,[44] at {15.5, 4.2}, corresponds to the structure of [MoO_2Br_2(bipy)], in which only one ligand deviates significantly from the axis of the octahedron.

F. Complexes with meridional tridentate ligands

Tridentate ligands spanning meridional positions, such as terpyridine, induce a double axial distortion **5** (average axial bond angles of 77.8°, standard deviation 2.1°). The symmetry measures calculated from the experimental structures of [M(terpy)$_2$] complexes are plotted in Fig. 14 together with the ideal line discussed above. It is seen that the behavior of all structures significantly deviate from the Bailar path (square root sums larger than 4.8 in all cases). Most of them (solid circles in Fig. 14) are in excellent agreement with the expected behavior for a double axial distortion. The deviation of some of the terpyridine complexes from the theoretical curve is due to the fact that the two M(terpy) planes form a dihedral angle that deviates from 90° by at least 1.4° (white circles in Fig. 14). Although it is out of the scope of this paper, it is

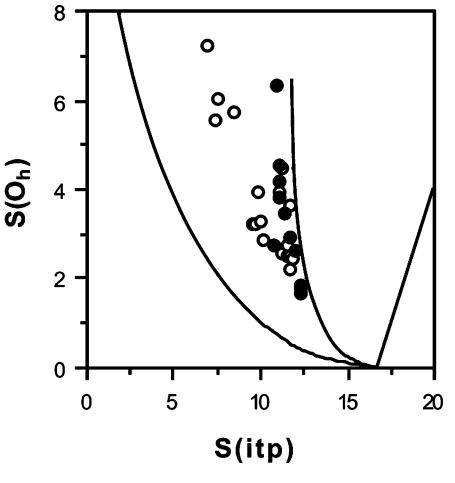

Fig. 14 Scatterplot of the octahedral and trigonal prismatic measures for a molecular model of double axial bending **5** (central solid line), and experimental data for complexes of the type [M(terpy)$_2$] with the two terdentate ligands practically perpendicular (dihedral angle 90.0° ± 1.4, black circles) or slightly twisted (white circles). The curves corresponding to the Bailar twist (leftmost solid line) and to the tetragonal Jahn–Teller distortion (rightmost straight line) are also plotted for reference.

interesting to note here that the coordination sphere of the metal atom in some minerals[45] appears aligned along the path expected for the double axial distortion of D_{2d} symmetry, much in the same way as the [M(terpy)$_2$] complexes.

G. Complexes with facial tridentate ligands

Facial tridentate ligands such as those depicted in **14** and **15** provide an interesting family of bis(tridentate) complexes from a structural viewpoint. The trigonal symmetry of these ligands, together with bite angles smaller than 90°, favor distortions of the octahedron to trigonal antiprisms (D_{3d} symmetry, **6**). However, one can find in these families molecules with a significant Bailar twist and also the bond stretch distortions characteristic of the Jahn–Teller effect in Cu(II) complexes. Hence, the quantitative symmetry analysis of their structures offers an excellent opportunity to test the ability of the CSM approach to detect the coexistence of different distortion modes in the same molecular structure.

First, we can identify those structures that show essentially a Bailar distortion only (square root sums of less than 4.5). We can see that none of these structures shows significant Jahn–Teller or trigonal-antiprismatic distortions from the octahedron, having $\alpha \geqslant 84°$ and $\Delta < 0.1$ Å, (Δ is the difference between the largest and shortest metal–ligand bond distances) and nicely follow the curve for the ideal Bailar path [Fig. 15(a)]. As for the structures that significantly deviate from the Bailar curve (square root sums $\geqslant 4.5$), we can classify them into two broad groups. The first group comprises those structures that show neither a Bailar twist ($\theta \geqslant 59°$) nor a Jahn–Teller distortion ($\Delta < 0.1$ Å), and fall along the expected line for elongated trigonal prisms [Fig. 15(b)]. In the second group we have a variety of structures that present two or more of the Bailar, Jahn–Teller and trigonal antiprismatic distortions [Fig. 15(c)]; these structures appear in the symmetry map between the two ideal lines, that is, a Jahn–Teller and trigonal antiprismatically distorted structure appears between the pure Jahn–Teller and TAP lines, whereas a structure with significant Bailar and trigonal antiprismatic distortions appears between the two leftmost lines shown in Fig. 15.

If we now select those structures that present twist angles $\theta \geqslant 59°$ and no significant Jahn–Teller distortion ($\Delta < 0.1$ Å), their symmetry measures align themselves along the model curve for the D_{3d} (trigonal antiprism) distortion [Fig. 15(b)].

Finally, a similar plot for those structures with significant Jahn–Teller distortions [Fig. 15(c)] shows that the symmetry values do not fit the model curve, clearly indicating that one or both of the two other distortions (Bailar twist and trigonal antiprism) coexist with the Jahn–Teller bond stretch in these compounds.

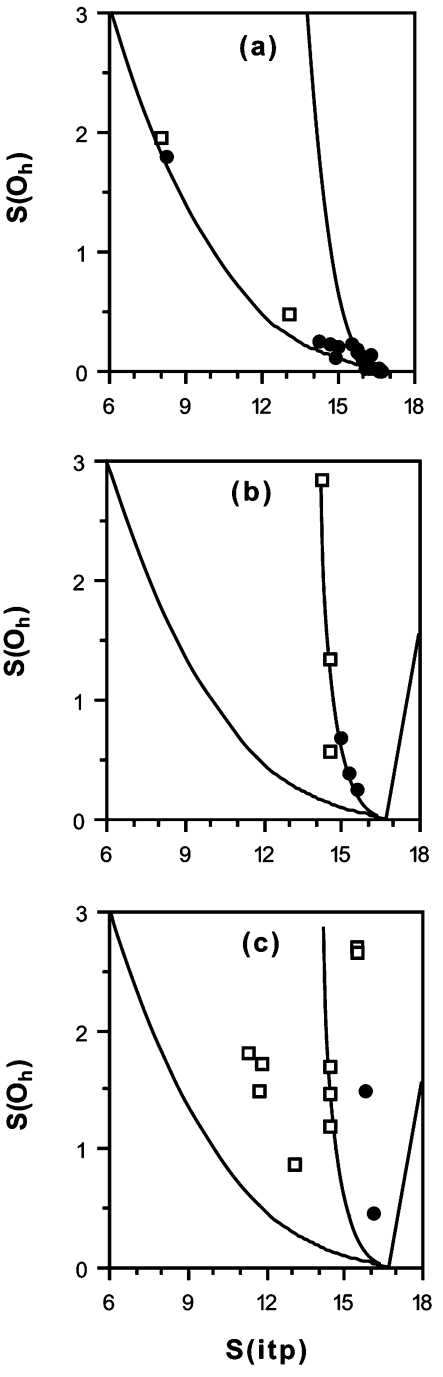

Fig. 15 Scatterplot of the octahedral and trigonal prismatic measures of tris(bidentate) complexes with ligands of types **14** (circles) and **15** (squares). The data shown correspond to complexes with square root sums of 4.5 or less (a); with only a D_{3d} distortion (b, characterized by $\alpha \geqslant 87°$ and $\theta \geqslant 59°$), and with combinations of Jahn–Teller, Bailar and bond angle distortions ($\alpha < 87°$, $\Delta \geqslant 0.1$ Å or $\theta < 59°$ (c). The solid lines shown correspond to the model distortions (from left to right) D_3 Bailar twist (Fig. 1), D_{3d} trigonal antiprism (**6**) and D_{4h} Jahn–Teller (**1**).

H. Hexagonal and pentagonal pyramidal complexes

Although these two structures are rare for hexacoordinated transition metal complexes, a few examples have been structurally characterized and are collected in Table 1 together with their octahedral and trigonal prismatic measures. The structures that appear in the symmetry map in the region around $S(O_h) = S(\text{itp}) \approx 33$ should be expected to be approximately hexagonal, according to the above model study of a distortion of the octahedron through a compressed trigonal antiprism (rule 8). The hexagonal character of such structures is verified by the small values of their C_6 symmetry measures (Table 1). It will be shown elsewhere that these complexes occupy the same position in the symmetry map as hexagonal supramolecular assemblies, thus showing the ability of the CSM approach to identify shapes independently of their nature or size (the hexagonal hexacoordinated complexes have edges of 2.3–2.5 Å, whereas the hexagonal supramolecular assemblies have edges between 2.8 and 4.7 Å).

The position occupied by a few complexes in the symmetry map, around {10, 22}, point to a pentagonal structure as found for model pentagonal pyramids (Fig. 3, PP), since only a severe skew trapezoidal distortion or a severely compressed trigonal prism could be expected to give similar symmetry measures (Figs. 3 and 4). This is nicely verified by the small values of their C_5 symmetry measures (Table 1).

Table 1 Symmetry measures for hexacoordinated complexes with hexagonal and pentagonal pyramidal structures

M	Donor set	Geometry	$S(O_h)$	S(itp)	$S(C_6)$	$S(C_5)$	Refcode	Ref.
Ni	P_6	hex	32.87	33.68	0.00	23.73	VOVZOV	46
Ni	As_6	hex	30.88	33.71	0.07	23.69	ZUDWUQ	47
Hg	N_5Cl	PP	26.41	12.05	25.79	2.14	GELKIR	48
Hg	N_3O_2I	PP	22.66	11.63	29.24	2.90	NEJXIJ	49
Ag	N_2O_4	PP	22.66	9.03	29.65	2.23	SENJIE	50
Y	N_3O_3	PP	19.99	12.44	24.40	2.92	QABQIJ	53
Ag	NO_5	PP	17.61	10.53	23.27	5.14	VARVIT	52
Hg	N_5Cl	PP	21.69	9.62	25.38	3.76	SERGOL	51

I. The skew-trapezoidal bipyramid

A recent report of an "unusual skew-trapezoidal bipyramidal geometry" for a hexacoordinated Re complex[54] prompted us to look at such distortion of the octahedron from the point of view of the symmetry measures. We have used a molecular model in which the equatorial ligands are gradually converted into a trapezoid by simultaneously increasing γ and decreasing η (**9**), whereas the axial ligands are bent away from the short edge of the trapezoid.

This distortion is represented in the symmetry map (Fig. 16) by a line close to that of the biaxial distortion (Fig. 3) discussed above. The calculated symmetry measures for the Re complex, {1.04, 14.25}, place this structure far away from the region of the skew-trapezoidal bipyramid model (the leftmost point on Fig. 16). Furthermore, this point is close to the Bailar line (square root sum 4.8) and the small value of S(itp) points to a distorted trigonal prismatic structure. The d^2 electron configuration of the metal ion in this complex and the small rotation angle between the two trigonal faces ($\theta = 6.4°$) are consistent with the structural and symmetry patterns for most d^0–d^2 complexes discussed above (sections **A** and **B**). In contrast, the symmetry measures for several Sn complexes, as well as for a couple of Hg and Cu compounds, that can be identified as skew-trapezoidal bipyramidal (see ESI for data) are fully consistent with the model curve, even if the strong bond distance distortions found experimentally have not been taken into account in our model.

J. Cyclotrienide complexes

The piano-stool cyclotrienide metal complexes **12** have one small trigonal face formed by the aromatic ring and a larger face formed by three monodentate ligands. Thus, the inequality of the two trigonal faces implies C_{3v} structures at twist angles of 0 and 60°. The former case has been analyzed above with a molecular model for a truncated trigonal pyramid (**9**). Furthermore, since the rotation of cyclotrienide around the trigonal axis is expected to be facile at room temperature it is worth looking at the evolution of the symmetry measures along that path. This is represented in Fig. 17, where such a rotation corresponds to a line parallel to the Bailar twist in the symmetry map. The experimental structures are consistent with the idealized path, appearing at the end of the curve corresponding to staggered structures (*i.e.*, pseudooctahedral).

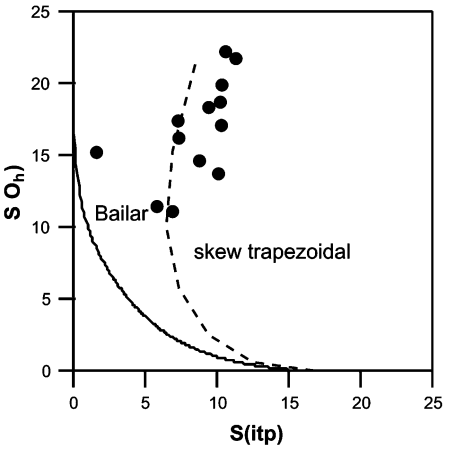

Fig. 16 Scatterplot of the octahedral and trigonal prismatic measures of a model hexacoordinated complex with skew-trapezoidal bipyramidal distortion **9** (dashed line) and experimental data for a Re complex[54] (leftmost circle) and for several Sn, Cu and Hg compounds (remaining circles, data provided as ESI). The Bailar path is also shown for reference (solid line).

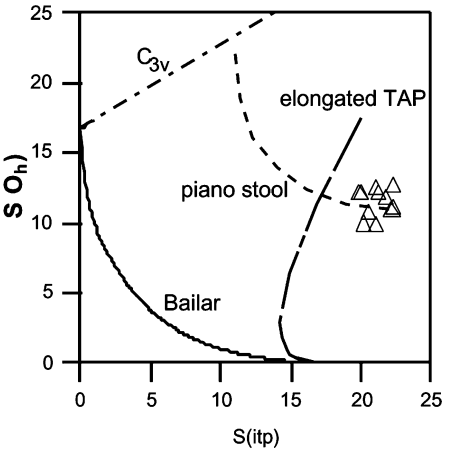

Fig. 17 Scatterplot of the octahedral and trigonal prismatic measures of a model piano-stool molecule $[M(C_3H_3)L_3]$ upon rotation of the C_3H_3 group around the trigonal axis (dashed line). The model lines corresponding to the D_3 Bailar twist (lower solid curve), D_{3d} elongated trigonal antiprisms (long dashed line), and C_{3v} truncated trigonal pyramid (leftmost dot-dashed line) are also shown for reference. The experimental data corresponding to $[M(C_3R_3)L_3]$ complexes are represented by triangles.

K. Capped trigonal prisms

We may wonder how close to the ideal polyhedron are the capped trigonal prisms that appear in heptacoordinated compounds. Two of the best examples of mono-capped trigonal prisms, according to the criterion of Maseras and Eisenstein,[55] are the $[MF_7]^{n-}$ anions of Zr(IV),[56] Nb(V)[57] and Ta(V),[58] as well as the $[Mo(CNBu)_6I]^+$ and $[Mo(CNBu)_7]^{2+}$ complexes.[59,60] If we analyze the prismatic core, thus omitting the capping ligand in these compounds, we find symmetry measures (Table 2) that indicate close proximity to an ideal trigonal prism [S(itp) $\leqslant$ 2.5], although distorted in a non-Bailar way (square root sums of 5.2 or higher), corresponding to the expansion of the capped tetragonal face.

Main conclusions

The present study has focused on the shape and symmetry measures of hexacoordinated transition metal complexes

Table 2 Structural data and symmetry measures of the prismatic core of heptacoordinated capped trigonal prismatic complexes

Compound	$S(O_h)$	S(itp)	Sum	Refcode	Ref.
$K_2[NbF_7]$	16.74	1.17	5.2		57
$K_2[TaF_7]$	16.95	1.19	5.2		58
$[Mo(CNBu)_6I]^+$	18.20	1.79	5.6	BUICMO	59
$[Mo(CNBu)_7]^{2+}$	18.64	2.47	5.9	IBICMO	60
$[ZrF_7]^{3-}$	16.94	1.18	5.2	ENFZRB10	56

relative to the octahedron and the trigonal prism. While the perfect octahedron is unequivocally defined (provided size and orientation are disregarded), an infinite number of trigonal prisms with D_{3h} symmetry exists. We have adopted a definition of an ideal trigonal prism (itp) with all its edges of the same length, thus having two equilateral triangles and three squares as faces. Such a definition of ideality is not only unique, but is also representative of the experimental structural data in transition metal homoleptic complexes with thiolato, alkyl or aryl ligands.

A symmetry map for hexacoordination can be built up by representing a scatterplot of the octahedricity and trigonal prismacity of model MX_6 cores for a variety of geometries. The limits of the chemically meaningful values in such a symmetry map are provided by the Bailar twist that interconverts the octahedron and the trigonal prism, the Jahn–Teller tetragonal distortion from a perfect octahedron and axial compression of an ideal trigonal prism. The Bailar curve in the symmetry map happens to be that of the minimum constant distance to the two reference shapes, the octahedron and the ideal trigonal prism. The square root sum of the two symmetry values is a constant along the Bailar pathway, the *Bailar symmetry constant*, and is equal to 4.16. Significant deviation of the square root sum of the symmetry measures from that symmetry constant indicates the existence of a non-Bailar distortion. Other regions of the symmetry map are usually indicative of the simultaneous existence of more than one distortion mode. However, angular distortions of the octahedron (*e.g.*, **3**, **4** and **6**) cannot be expected to give S(itp) values smaller than about 8. Following the analysis of a variety of distortions in model molecules, a set of rules has been deduced that give information on the type of distortions that may be present in a given molecular structure. A summary of the expected values of octahedral and trigonal prismatic symmetry measures that can be expected for different geometries of six vertex polyhedra is presented in Table 3, together with the examples analyzed in this paper or in forthcoming papers devoted to extended solids and to clusters and supramolecular assemblies.

The analysis of the experimental structural data for several families of hexacoordinated compounds with mono-, bi- and tridentate ligands shows that most of the structures are aligned along the Bailar path (*i.e.*, they correspond to *trigonal metaprisms*) with small deviations (within 2 units) due to the presence of other distortion modes. Only strong bond stretch distortions of the Jahn–Teller type (distance differences larger than 0.7 Å), the pentagonal pyramid or the hexagon produce large deviations from the pure Bailar line of the symmetry map. Those structures that are significantly twisted from the octahedron ($\theta < 40°$) correspond to metal ions with d^0 to d^2 electron configurations, whereas all complexes with d^3 to d^{10} configurations are characterized by $\theta \geqslant 40°$. For Cu(II) complexes, many structures show evidence of combined Bailar twist and JT distortion, but three structures of nearly trigonal prismatic Cu(II) complexes [S(itp) < 3] have been detected.

For tris(chelated) complexes two different trends are found. A group of compounds shows a simple linear dependence between the normalized bite and the twist angle, whereas other families of structures present normalized bites of around 1.3, nearly independent of the twist angle. We conclude that a trigonal prismatic structure exists only if the normalized bite is 1.34 or less and the electron configuration is adequate (d^0, d^1, or high-spin d^5), although the latter requirement may be relaxed for Werner-type complexes (especially with O-donor ligands). Hexadentate encapsulating ligands show a behavior similar to that found for tris(chelated) complexes with ligands such as ethylenediamine or β-diketonates, those with nearly trigonal prismatic structures being d^0, d^1, or high-spin Fe(III) d^5 complexes.

Less common shapes, such as the hexagon or the pentagonal pyramid, appear in specific regions of the octahedron-itp symmetry map. Hence, the planar hexagon has symmetry measures calculated for a model hexacoordinated molecule {33.7, 33.3}, while the pentagonal pyramids appear on the symmetry map distributed in a practically linear way between the {16, 29} and {32, 19} points. The hexagonal character of several experimental structures is verified by their C_6 symmetry measures. Similarly, the pentagonal pyramidal geometry of several molecules close to the {10, 22} point has been verified by their C_5 symmetry measures.

One of the interesting properties of the symmetry measures employed is that they can be applied to diverse systems regarding composition and size. Hence, we plan to carry out a study of the application of the reported symmetry map to the

Table 3 Ranges of $S(O_h)$ and S(itp) values for six-vertex polyhedra with different geometries, and some examples of experimental ML_6 structures

Geometry[a]	Subgroup	$S(O_h)$	S(itp)	Examples
Metaprisms [Bailar, Fig. 1, eqn. (3)]	D_6	0–17.3	0–17.3	$[MMe_6]$, $[M(SR)_6]$, [M(bidentate)$_3$]
Compressed TAP (**6**, $\alpha > 90°$)	D_{3d}	0–27[b]	16–30[b]	Supramolecular M_6 assemblies
Elongated TAP (**6**, $\alpha < 90°$)	D_{3d}	0–10[c]	14–18[b]	[M(tridentate)$_2$]
Axial (**4**)	C_{2v}	0–20	17–6	*cis*-$[Mo^{VI}O_2L_4]$
Double-axial (**5**)	D_{2d}	0–18	17–11.5	[M(terpy)$_2$], anatase
Skew-trapezoidal (**9**)	C_{2v}	0–30[d]	12–17[d]	*trans*-[Sn(bidentate)$_2$(CH$_3$)$_2$]
Equatorial bending (**3**)	D_{2h}	0–5[e]	16–18[e]	*trans*-[ML$_2$(bidentate)$_2$]
Jahn–Teller (**1**) [eqn. (6)]	D_{4h}	0–8	16–23	Cu(II) complexes
Rhombic bipyramid (**8**)	D_{2h}	0–5	16–18	
Elongated TP (**7**, $\alpha < 8.18°$)	D_{3h}	16.7–27[f]	0–11[f]	[M(Pc)L$_2$] early transition metals
Compressed TP (**7**, $\alpha > 81.8°$)	D_{3h}	16.7–50[g]	0–43[g]	
Truncated trig. pyr. (**9**) [eqn. (13)]	C_{3v}	16.7–35	0–35	[M(C$_3$R$_3$)L$_3$]
Linear chain	$D_{\infty h}$	66.7	60.4	
Hexagon	D_{6h}	~33	~33	[Ni(P$_6$^{t}Bu$_6$)]
Pentagonal pyramid	C_{5v}	29–32	16–19	See Table 1

[a] TP = trigonal prism, TAP = trigonal antiprism. [b] $90 < \alpha < 120°$ [Fig. 4(*a*)]. [c] $60 < \alpha < 90°$ [Fig. 4(*a*)]. [d] $0 < \delta < 35°$ [Fig. 4(*b*)]. [e] $60 < \lambda < 90°$ [Fig. 4(*d*)]. [f] $\alpha = 51°$, $f/h = 2.00$. [g] Values corresponding to two superimposed triangles.

analysis of the structures of systems such as extended solids and minerals, hexametallic clusters and hexanuclear supramolecular assemblies of transition metals linked by bridging ligands.

Acknowledgements

This work has been supported by the Dirección General de Enseñanza Superior (DGES), project PB98-1166-C02-01; Comissió Interdepartamental de Ciència i Tecnologia (CIRIT), grant SGR99-0046, the US-Israel Binational Science Foundation (Grant 1998077) and the Israel Science Foundation (Grant 30/01). Inspiration from discussions with K. Hegetschweiler is gratefully acknowledged.

References

1 H. Zabrodsky, S. Peleg and D. Avnir, *J. Am. Chem. Soc.*, 1992, **114**, 7843.
2 S. K. Kang, T. A. Albright and O. Eisenstein, *Inorg. Chem.*, 1989, **28**, 1613.
3 W. K. Kang, H. Tang and T. A. Albright, *J. Am. Chem. Soc.*, 1993, **115**, 1971.
4 M. Shen, H. F. Schaefer III and H. Partridge, *J. Chem. Phys.*, 1992, **98**, 508.
5 F. Maseras, A. Lledós, E. Clot and O. Eisenstein, *Chem. Rev.*, 2000, **100**, 601.
6 A. Haaland, A. Hammel, K. Rypdal and H. V. Volden, *J. Am. Chem. Soc.*, 1990, **112**, 4547.
7 S. Kleinhenz, M. Schubert and K. Seppelt, *Chem. Ber.*, 1997, **130**, 903.
8 S. Kleinhenz, V. Pfennig and K. Seppelt, *Chem. Eur. J.*, 1998, **4**, 1687.
9 P. M. Morse and G. S. Girolami, *J. Am. Chem. Soc.*, 1989, **111**, 4114.
10 V. Pfennig and K. Seppelt, *Science*, 1996, **271**, 626.
11 J. C. Bailar, Jr., *J. Inorg. Nucl. Chem.*, 1958, **8**, 165.
12 E. L. Muetterties and L. J. Guggenberger, *J. Am. Chem. Soc.*, 1974, **96**, 1748.
13 D. Avnir, O. Katzenelson, S. Keinan, M. Pinsky, Y. Pinto, Y. Salomon, and H. Zabrodsky Hel-Or, in *CSM: Conceptual Aspects*, ed. D. H. Rouvray, Taunton, England, 1997.
14 S. Alvarez and M. Llunell, *J. Chem. Soc., Dalton Trans.*, 2000, 3228.
15 S. Alvarez, M. Pinsky and D Avnir, *Eur. J. Inorg. Chem.*, 2001, 1499.
16 S. Alvarez, M. Pinsky, M. Llunell and D. Avnir, *Cryst. Eng.*, 2001, **4**, 179.
17 O. Katznelson, J. Edelstein and D. Avnir, *Tetrahedron: Asymmetry*, 2000, **11**, 2695.
18 S. Keinan and D. Avnir, *J. Chem. Soc., Dalton Trans.*, 2001, 941.
19 H. Zabrodsky and D. Avnir, *J. Am. Chem. Soc.*, 1995, **117**, 462.
20 H. Zabrodsky, S. Peleg and D. Avnir, *J. Am. Chem. Soc.*, 1993, **115**, 8278 (erratum: 1994, **116**, 656).
21 W. A. Dollase, *Acta Crystallogr. Sect. A*, 1974, **30**, 513.
22 A. Holden, *Shapes, Space and Symmetry*, Columbia University Press, New York, 1971.
23 M. Pinsky and D. Avnir, *J. Math. Chem.*, 2001, **30**, 109.
24 M. O'Keeffe and B. G. Hyde, *Crystal Structures. I. Patterns and Symmetry*, Mineralogical Society of America, Washington, DC, 1996.
25 S. Keinan and D. Avnir, *Inorg. Chem.*, 2001, **40**, 318.
26 P. Alemany and S. Alvarez, to be submitted.
27 D. L. Kepert, *Inorganic Stereochemistry*, Springer Verlag, Heidelberg, 1982.
28 T. M. Greaney, C. L. Raston, A. H. White and E. N. Maslen, *J. Chem. Soc., Dalton Trans.*, 1975, 876.
29 T. M. Garrett, T. J. McMurry, M. W. Hosseini, Z. E. Reyes, F. E. Hahn and K. N. Raymond, *J. Am. Chem. Soc.*, 1991, **113**, 2965.
30 T. B. Karpishin, T. D. P. Stack and K. N. Raymond, *J. Am. Chem. Soc.*, 1993, **115**, 182.
31 T. J. Anderson, M. A. Neuman and G. A. Melson, *Inorg. Chem.*, 1973, **12**, 927.
32 T. W. Hambley, C. J. Hawkins and T. A. Kabanos, *Inorg. Chem.*, 1987, **26**, 3740.
33 B. Morosin and H. Montgomery, *Acta Crystallogr., Sect. B*, 1969, **25**, 1354.
34 F. Sanz-Ruiz, S. Martínez-Carrera and S. García-Blanco, *An. R. Soc. Esp. Fís. Quím., Ser. A*, 1970, **66**, 309.
35 U. Thewalt and T. Adam, *Z. Naturforsch., B: Anorg. Chem. Org. Chem.*, 1978, **33**, 142.
36 A. Gleizes, S. Sans-Lenain, D. Medus, N. Hovnanian, P. Miele and J.-D. Foulon, *Inorg. Chim. Acta*, 1993, **209**, 47.
37 S. A. Gromilov, I. A. Baidina, S. A. Prokhorova and P. A. Stabnikov, *Zh. Strukt. Khim.*, 1995, **36**, 541.
38 A. von Zelewsky, *Stereochemistry of Coordination Compounds*, J. Wiley, Chichester, 1996.
39 X.-H. Bu, X.-C. Cao, W.-Q. Zhang, R.-H. Zhang and T. Clifford, *Transition Metal Chem. (London)*, 1997, **22**, 513.
40 X.-H. Bu, W. Chen, Y.-Y. Fang, S.-L. Lu, C.-F. Wang and R.-H. Zhang, *Acta Chem. Scand.*, 1998, **52**, 813.
41 D. Funkemeier and R. Mattes, *J. Chem. Soc., Dalton Trans.*, 1993, 1313.
42 A. Dolbecq, E. Cadot, D. Eisner and F. Secheresse, *Inorg. Chem.*, 1999, **38**, 4127.
43 M. Albrecht, S. J. Franklin and K. N. Raymond, *Inorg. Chem.*, 1994, **33**, 5785.
44 R. H. Fenn, *J. Chem. Soc. A*, 1969, 1764.
45 S. Alvarez and D. Avnir, to be submitted.
46 R. Ahlrichs, D. Fenske, H. Oesen and U. Schneider, *Angew. Chem., Int. Ed. Engl.*, 1992, **31**, 323.
47 E. Hey-Hawkins, M. Pink, H. Oesen and D. Fenske, *Z. Anorg. Allg. Chem.*, 1996, **622**, 689.
48 G. Chessa, G. Marangoni, B. Pitteri, V. Bertolasi, V. Ferretti and G. Gilli, *J. Chem. Soc., Dalton Trans.*, 1988, 1479.
49 J. Pickardt and S. Wiese, *Z. Naturforsch., B: Chem. Sci.*, 1997, **52**, 847.
50 C. A. Reiss, K. Goubitz and D. Heijdenrijk, *Acta Crystallogr., Sect. C*, 1990, **46**, 1089.
51 G. Chessa, G. Marangoni, B. Pitteri, V. Bertolasi, V. Ferretti and G. Gilli, *J. Chem. Soc., Dalton Trans.*, 1990, 915.
52 M. J. Kronenburg, C. A. Reis, K. Goubitz and D. Heijdenrijk, *Acta Crystallogr., Sect. C*, 1989, **45**, 1361.
53 H. W. Gorlitzer, M. Spiegler and R. Anwander, *Eur. J. Inorg. Chem.*, 1998, 1009.
54 G. Bandoli, A. Dolmella, T. I. A. Gerber, J. Perils and J. G. H. du Prez, *Inorg. Chim. Acta*, 2000, **303**, 24.
55 F. Maseras and O. Eisenstein, *New J. Chem.*, 1997, **21**, 961.
56 I. P. Kondratyuk, B. V. Bukvetskii, R. L. Davidovich and M. A. Medkov, *Koord. Khim.*, 1982, **8**, 218.
57 G. M. Brown and L. A. Walker, *Acta Crystallogr.*, 1966, **20**, 220.
58 C. C. Torardi, L. H. Brixner and G. Blasse, *J. Solid State Chem.*, 1987, **67**, 21.
59 D. F. Lewis and S. J. Lippard, *Inorg. Chem.*, 1972, **11**, 621.
60 D. F. Lewis and S. J. Lippard, *J. Am. Chem. Soc.*, 1975, **97**, 2697.